Maejo Int. J. Sci. Technol. **2010**, *4*(03), 468-482

Maejo International Journal of Science and Technology

ISSN 1905-7873
Available online at www.mijst.mju.ac.th

Full Paper

Natural convection of nanofluids in a cavity with linearly varying wall temperature

Sivanandam Sivasankaran [1, *], Thangaraj Aasaithambi [2] and Subbarayagounder Rajan [3]

[1] University College, Sungkyunkwan University, Suwon 440-746, South Korea
[2] Department of Mathematics, Sengunthar Engineering College, Tiruchengode – 637205, India
[3] Department of Mathematics, Erode Arts and Science College, Erode – 638 009, Tamilnadu, India

* Corresponding author, e-mail: sd.siva@yahoo.com

Received: 28 April 2010 / Accepted: 16 July 2010 / Published: 26 November 2010

Abstract: The aim of the present numerical study is to investigate the convective flow and heat transfer behaviour of nanofluids with different nano-particles in a square cavity. The hot left wall temperature of the cavity is varied linearly with height whereas the cold right wall temperature is kept constant. The finite volume method is used to discretise the transport equations, which are solved by iterative method. Numerical simulations are carried out for different combinations of pertinent parameters involved in the study. It is found that the heat transfer rate increases on increasing the volume fraction of the nanofluid for all types of nanoparticles considered. The increment in average Nusselt number is strongly dependent on the nanoparticle chosen.

Keywords: convective heat transfer, nanofluid, linearly varying wall temperature

---

Nomenclature

c_p	specific heat, J/(kg·K)
F_o	dimensionless time
g	acceleration due to gravity, m/s^2
h	heat transfer coefficient
k	thermal conductivity, W/(m·K)
L	size of enclosure, m
Nu	local Nusselt number
$\overline{Nu}$	average Nusselt number
Pr	Prandtl number, ν_f/α_f

Maejo Int. J. Sci. Technol. **2010**, *4*(03), 468-482

p	Pressure, Pa
Ra	Rayleigh number, $\dfrac{g\beta_f(\theta_h-\theta_c)L^3}{\nu_f\alpha_f}$
T	dimensionless temperature
t	time, s
u, v	velocity components, m/s
U, V	dimensionless velocity components
x, y	Cartesian coordinates
X, Y	dimensionless coordinates

Greek symbols

α	thermal diffusivity, m^2/s
β	volumetric coefficient of thermal expansion, 1/K
ε	heat transfer coefficient ratio
ϕ	volume fraction of nanofluid
μ	dynamic viscosity, Pa·s
ν	kinematic viscosity, μ_f/ρ_f
ρ	density, kg/m^3
θ	temperature, K
ψ	dimensionless stream function

Subscripts

c	cold wall
e	effective
h	hot wall
f	base fluid
n	nanofluid
p	nanoparticle

Superscript

*	property ratio

INTRODUCTION

Convective heat-transfer cooling enhancement technique has been a major problem in engineering and technological applications due to thermal management of small devices. The efficacy of such cooling process is restricted by poor thermal properties of the working medium. A better heat transfer medium is needed for the convective heat transfer technique to overcome this limitation. Recently, fluids with nanometre-sized particles suspended in them, called nanofluids, first termed by Choi and Eastman [1], have been considered. Much work has been conducted to study the physical properties of nano-particles but little studied is the convective heat transfer of nanofluids in enclosures [2-5]. Before using nanofluids in practical applications, an investigation on convective heat transfer technique is needed in detail. In the present work, a numerical study is conducted to investigate the heat transfer and fluid flow characteristics of nanofluids inside an enclosure.

Some researchers analysed the convective heat transfer of nanofluids by considering different models of nanofluid properties in an enclosure. Khanafer et al. [6] numerically investigated the buoyancy-driven convection in a two-dimensional enclosure filled with nanofluids. They found that the heat transfer rate increases with an increase in the nanoparticle volume fraction. Jou and Tzeng [7] performed a numerical study on the effect of small aspect ratio on the natural convection of nanofluids in a rectangular enclosure. They found that the average Nusselt number at the hot wall increases as the aspect ratio decreases. Wen and Ding [8] made an experimental study on heat transfer using titanium-dioxide-based nanofluid. The results showed that the presence of the nanoparticles decreases the convective heat transfer rate. Hwang et al. [9] studied theoretically the thermal characteristics of natural convective heat transfer of water-based Al_2O_3 nanofluid in a rectangular cavity. They used two different models to calculate the effective viscosity of the nanofluid and compare the results obtained from these models. They showed that the ratio of the heat transfer coefficient of the nanofluid to that of the base fluid decreases as the size of the nanoparticles increases.

Ho et al. [10] numerically studied the effects of uncertainty in the effective viscosity and thermal conductivity of nanofluids on convection in an enclosure. They concluded that the effective dynamic viscosity should be taken into account when studying the heat transfer efficacy of natural convection in enclosures. Abu-Nada et al. [11] studied natural convection in horizontal concentric annuli filled with nanofluids containing various nanoparticles. Similar investigation in a partially heated rectangular enclosure was numerically studied by Oztop and Abu-Nada [12]. They found that the enhancement of the heat transfer is more pronounced at low aspect ratio than at high aspect one. Santra et al. [13] numerically studied natural convection of nanofluids in a differentially heated square cavity. They treated the nanofluids as non-Newtonian. Ghasemi and Aminossadati [14] showed that the heat transfer rate is maximised at a specific inclination angle depending on the Rayleigh number and the volume fraction of nanoparticles when studying the convection in an inclined enclosure filled with water-CuO nanofluid.

In most of the numerical or experimental studies on convective heat transfer of nanofluids, researchers have considered the cavity with either isothermal or isoflux thermal boundary conditions for vertical walls. However, these thermal boundary conditions are not suitable in many applications such as heat exchangers, injection moldings and solidification processes. We need the knowledge of the effect of variable wall temperature for some applications. Hossain and Wilson [15] performed a numerical study to investigate the natural convection in a porous enclosure with internal heat generation under linearly varying temperature boundary condition. Laminar natural convection in a two-dimensional square cavity with non-uniform side-wall temperature was studied numerically by Saeid and Yaacob [16]. They found that the average Nusselt number varies based on the hot-wall temperature. Sathiyamoorthy et al. [17] numerically investigated natural convection flow in a square cavity with linearly heated vertical walls and uniformly heated bottom wall. Dare and Petinrin [18] studied the natural convective flow along isothermal plates and in channels using diffusion velocity method. They found that as the wall temperature increases while keeping the mainstream fluid temperature constant, the thermal boundary layer thickness increases.

The above-mentioned studies are concerned with convection in enclosures with fluids or fluid-saturated porous medium with variable boundary conditions. No work seems to have been carried out on convective flow of nanofluids for such thermal boundary conditions. Therefore, the present study aims to investigate the effect of natural convective heat transfer and fluid flow characteristics in a square cavity with linearly varying hot-wall temperature utilising nanofluids.

MATHEMATICAL ANALYSIS

Consider a two-dimensional square cavity of size L filled with water-based nanofluid containing nanoparticles as shown in Figure 1. The left vertical wall of the cavity is heated linearly with height while the right vertical wall is cooled at a constant temperature and the horizontal walls are insulated. The nanofluid in the enclosure is a solid-liquid mixture with uniform volume fraction ϕ, shape and size of nanoparticles dispersed in base fluid water. Various nanoparticles, viz. Al_2O_3, Cu, Ag and TiO_2, are used in the study. The flow is assumed to be incompressible and laminar. It is also assumed that both the nanoparticles and the base fluid are in thermally equilibrium. The Boussinesq approximation is valid for the buoyancy term and all other thermophysical properties are assumed to be constant. In addition, the viscous dissipation is assumed to be negligible.

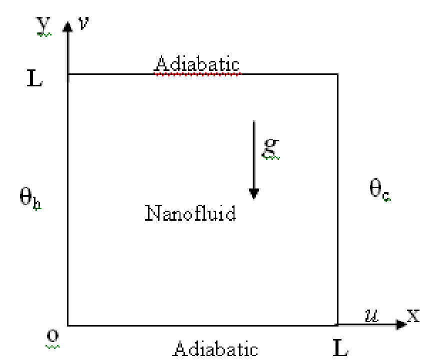

Figure 1. Physical configuration and coordinate system of a two-dimensional square cavity

The mathematical model for fluid flow and heat transfer for the above-mentioned geometrical and physical conditions and assumptions in non-dimensional form can be written as follows.

$$\frac{\partial U}{\partial X}+\frac{\partial V}{\partial Y}=0 \tag{1}$$

$$\frac{\partial U}{\partial Fo}+U\frac{\partial U}{\partial X}+V\frac{\partial U}{\partial Y}=-\frac{\partial P}{\partial X}+\Pr_f\left(\frac{C^*_{p,nf}\mu^*_{nf}}{k^*_{nf}}\right)\left[\frac{\partial^2 U}{\partial X^2}+\frac{\partial^2 U}{\partial Y^2}\right] \tag{2}$$

$$\frac{\partial V}{\partial F_O}+U\frac{\partial V}{\partial X}+V\frac{\partial V}{\partial Y}=-\frac{\partial P}{\partial Y}+\Pr_f\left(\frac{C^*_{p,nf}\mu^*_{nf}}{k^*_{nf}}\right)\left[\frac{\partial^2 V}{\partial X^2}+\frac{\partial^2 V}{\partial Y^2}\right]+Ra_f\Pr_f\beta^*_{nf}\left(\frac{\rho^*_{nf}C^*_{p,nf}}{k^*_{nf}}\right)^2 T \tag{3}$$

$$\frac{\partial T}{\partial Fo}+U\frac{\partial T}{\partial X}+V\frac{\partial T}{\partial Y}=\left[\frac{\partial}{\partial X}\left(k^*_{en}\frac{\partial T}{\partial X}\right)+\frac{\partial}{\partial Y}\left(k^*_{en}\frac{\partial T}{\partial Y}\right)\right] \tag{4}$$

The physical property ratios present in equations (2-4) are as follows: $k_{nf}^* = \dfrac{k_n}{k_f}$, $k_{en}^* = \dfrac{k_e}{k_n}$, $\mu_{nf}^* = \dfrac{\mu_n}{\mu_f}$, $c_{p,nf}^* = \dfrac{c_{p,n}}{c_{p,f}}$, $\rho_{nf}^* = \dfrac{\rho_n}{\rho_f}$ and $\beta_{nf}^* = \dfrac{\beta_n}{\beta_f}$, where the subscripts n and f denote, respectively, the nanofluid and the base fluid. Moreover, k_e denotes the effective thermal conductivity associated with possible heat transfer enhancement mechanisms of the nanofluid such as Brownian motion, liquid layering at liquid/particle interface, and phonon movement in nanoparticles.

The effective thermophysical properties of a nanofluid can be evaluated using various formulae available in the literature. The formulae selected for the thermophysical properties of the nanofluid in the present study are as follows [10], and the thermophysical properties of the base fluid (water) and various nanoparticles are presented in Table 1.

Density: $$\rho_n = (1-\phi)\rho_f + \phi\rho_p \tag{5}$$

Thermal expansion coefficient: $$\beta_n = \frac{1}{\rho_n}\left[(1-\phi)\rho_f\beta_f + \phi\rho_p\beta_p\right] \tag{6}$$

Specific heat: $$c_{p,n} = (1-\phi)c_{p,f} + \phi c_{p,p} \tag{7}$$

Thermal conductivity: This is evaluated from the well-known Maxwell formula [10] as

$$k_n = k_f\left[\frac{2 + k_{pf}^* + 2\phi(k_{pf}^* - 1)}{2 + k_{pf}^* - \phi(k_{pf}^* - 1)}\right] \tag{8}$$

with $k_{pf}^* = \dfrac{k_p}{k_f}$.

Dynamic viscosity: The Brinkman's formula [19] is used for the effective dynamic viscosity of a nanofluid, which is expressed as

$$\mu_n = \mu_f(1-\phi)^{-2.5} \tag{9}$$

The initial and boundary conditions in the dimensionless form are:

$F_o = 0$;	U=V = T =0	at	$0 \le X \le 1$ and $0 \le Y \le 1$
$F_o > 0$;	U=V = 0, $\dfrac{\partial T}{\partial Y} = 0$	at	Y = 0 and 1
	U=V = 0, T = Y	at	X = 0 and $0 \le Y \le 1$
	U=V = 0, T = 0	at	X = 1 and $0 \le Y \le 1$

Maejo Int. J. Sci. Technol. **2010**, *4*(03), 468-482

Table 1. Thermophysical properties of base fluid (water) and various nanoparticles [10-11]

Property	Base fluid	Nanoparticles			
	Water	Alumina (Al_2O_3)	Copper (Cu)	Silver (Ag)	Titanium oxide (TiO_2)
Density (ρ)	997.1	3970	8933	10500	4250
Specific heat (Cp)	4179	765	385	235	686.2
Thermal conductivity (k)	0.613	40	401	429	8.9538
Coefficient of thermal expansion ($\beta\times10^{-5}$)	21	0.85	1.67	1.89	0.9
Thermal diffusivity ($\alpha\times10^{7}$)	1.47	131.7	1163.1	1738.6	30.7

The following non-dimensional variables are used: $(X, Y) = (x, y)/L$, $(U, V) = (u, v)L/\alpha_n$, $Fo = t\alpha_n/L^2$, $P = pL^2/(\rho_n\alpha^2_n)$ and $T = (\theta - \theta_c)/(\theta_h - \theta_c)$. The non-dimensional numbers appearing in the above equations are: Ra (Rayleigh number) $= \dfrac{g\beta_f(\theta_h - \theta_c)L^3}{\nu_f\alpha_f}$ and Pr (Prandtl number) $= \nu_f/\alpha_f$. The stream function is calculated using $U = \dfrac{\partial\Psi}{\partial Y}$ and $V = -\dfrac{\partial\Psi}{\partial X}$. The heat transfer rate at the hot wall of the cavity is presented by means of the Nusselt number, which is evaluated as follows: $Nu_h = \dfrac{h_n L}{k_f} = -k^*_{nf}\left.\dfrac{\partial T}{\partial Y}\right|_{X=0}$. The average Nusselt number along the hot wall is obtained by integrating the local Nusselt number over the hot wall:

$$\overline{Nu} = \int_0^1 Nu_h dY. \tag{10}$$

In addition, it is also important to quantify the heat transfer efficacy of the nanofluid compared to that of the base fluid. The ratio of the average heat transfer coefficient of the nanofluid at the hot wall to that of the base fluid, ε_h, is calculated as

$$\varepsilon_h = \overline{h_n}\Big/\overline{h_f} \,. \tag{11}$$

METHOD OF SOLUTION

Numerical Method

The non-dimensional governing equations, together with boundary conditions, are discretised by implicit finite volume method, which is explained by Patankar [20]. The QUICK scheme is used for the convection terms and the central difference scheme is used for diffusion terms. The velocity and pressure are coupled by SIMPLE algorithm [20]. The solution domain is discretised with non-uniform mesh in both X and Y directions [10]. The grids are clustering towards the walls of the cavity. The effect of grid size is tested to select the appropriate grid density among a range from 41×41 to 161×161

Maejo Int. J. Sci. Technol. **2010**, *4*(03), 468-482

for Ra $=10^6$, Pr = 6.7 and constant fluid properties; see Figure 2. It is observed from the grid independence test that an 81×81 grid is enough to investigate the problem. The time step is chosen to be uniform, $\nabla F_0=10^{-5}$. The resulting algebraic equations are solved by iterative method. The iterations are stopped when the convergence criterion $\left|\frac{\varphi_{(n+1)}(i,j)-\varphi_{(n)}(i,j)}{\varphi_{(n+1)}(i,j)}\right| \le 10^{-6}$ is met for all variables $\varphi(=U, V, T)$.

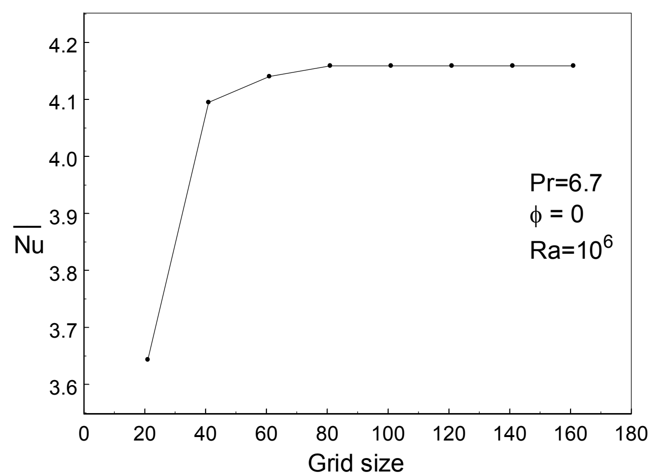

Figure 2. Grid independent test

Code Validation

The validation of present computational code for this study is verified against the existing results available in the literature. Simulations are carried out for natural convection in a differentially heated square cavity with isothermal walls for Rayleigh number ranging from 10^3 to 10^6 to validate the present code. The results obtained from the present code are compared with those by Khanafer et al. [6], Ho et al. [10], de Vahl Davis [21], Hadjisophocleous et al. [22], Fusegi et al. [23] and Barakos et al. [24] (Table 2). It is clearly seen from the table that the computed results are good agreement with the solutions available in the literature.

Table 2. Comparison of present results (average Nusselt number) with existing ones available in the literature

Ra	$\overline{Nu}$						
	Present	Khanafer et al. [6]	Ho et al. [10]	Davis [21]	Hadjisophocleous et al. [22]	Fusegi et al. [23]	Barakos et al. [24]
10^3	1.118	1.118	1.118	1.118	1.141	1.106	1.114
10^4	2.281	2.245	2.246	2.238	2.290	2.302	2.245
10^5	4.728	4.522	4.522	4.509	4.964	4.646	4.510
10^6	8.959	8.826	8.825	8.817	10.390	9.012	8.806

Maejo Int. J. Sci. Technol. **2010**, *4*(03), 468-482

RESULTS AND DISCUSSION

A numerical study is performed to investigate the natural convective flow and heat transfer characteristics of water-based nanofluids with various nanoparticles of different volume fractions in a cavity. The value of Prandtl number for the base fluid (water) is taken to be 6.7. Computations are carried out for the Rayleigh number ranging from 10^3 to 10^6, and the volume fraction ϕ of nanoparticles between 0-4%. The results obtained are discussed under different combinations of pertinent parameters involved in the study. Figure 3 shows a comparison of average Nusselt number of isothermal and linearly varying hot walls using pure fluid and Al_2O_3 nanofluid with volume fraction ϕ=0.04. It is clearly seen from the figure that there is much difference in the heat transfer rate of the linearly varying hot wall and the isothermal wall. The difference in the average Nusselt number between the two boundary conditions increases with increasing Rayleigh number.

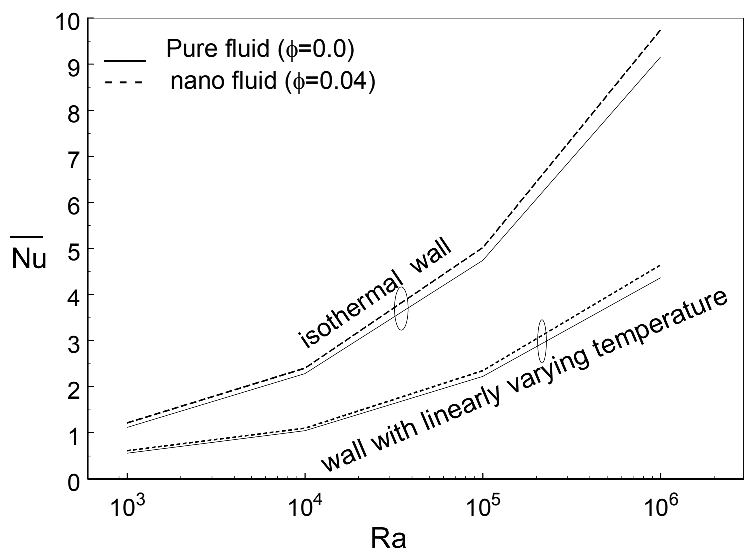

Figure 3. Average Nusselt number of isothermal wall and linearly varying hot wall using pure fluid and Al_2O_3 nanofluid with ϕ= 0.04

Though four types of nanoparticles are used, the illustrated figures for isotherms and streamlines with different values of Rayleigh number are provided only for Al_2O_3 nanofluid for brevity of the paper. Figure 4 shows fluid flow and heat transfer characteristics of Al_2O_3 nanofluid and pure fluid (water) for different values of Rayleigh number. The flow pattern consists of a single cell occupying the whole cavity. The core region of the cell is at the middle of the enclosure when $Ra \leq 10^4$. The isotherms are distributed almost equally throughout the enclosure. Here, convection is weakened and conduction is the dominant mode of heat transfer. The core region of the nanofluid is reduced compared to pure fluid for all values of Rayleigh number. When the Rayleigh number increases, the core region of the cell moves towards the cold wall and elongates. The corresponding isotherms show a vertical temperature stratification in the core region of the cavity. The core region moves towards the top-right corner of the enclosure when $Ra \geq 10^5$. The isotherms cluster along the thermally active walls and form thermal boundary layers.

Maejo Int. J. Sci. Technol. **2010**, *4*(03), 468-482

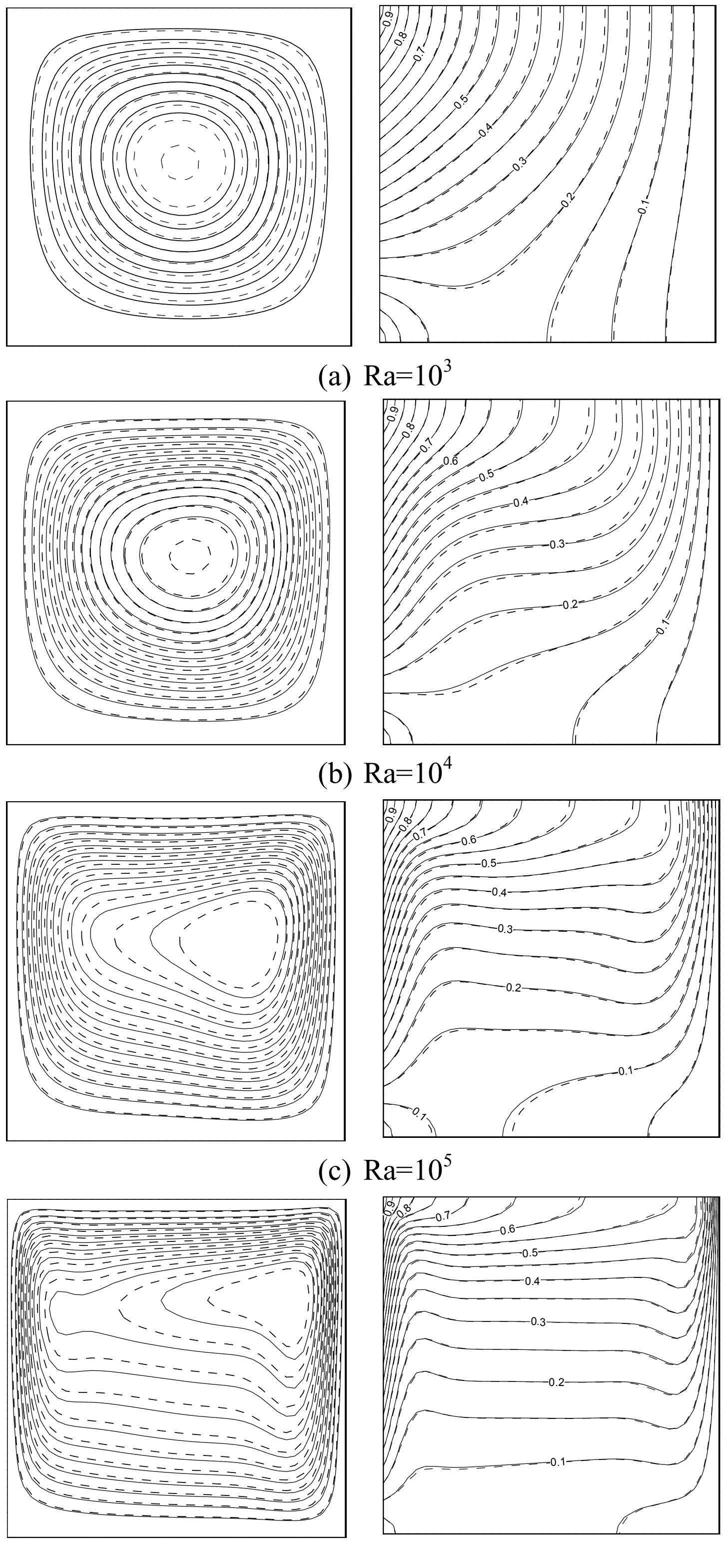

(a) Ra=10^3

(b) Ra=10^4

(c) Ra=10^5

(d) Ra=10^6

Figure 4. Streamlines (left) and isotherms (right) for different values of Rayleigh number (solid lines for pure fluid; dash lines for Al_2O_3 nanofluid:) with ϕ= 0.04

The fluid flow pattern for different nanofluids are depicted in Figure 5 for Ra=10^6. It is clearly seen from these figures that nanofluids with oxide nanoparticles have similar behaviour and nanofluids with metal particles have very similar flow patterns. Figure 6 shows the isotherm contours for different nanofluids with Ra=10^6 and ϕ=4%. The isotherms cluster near the thermally active walls and resemble the convection-dominated mode of heat transfer. On further scrutiny of these figures, there is not much difference in the heat distribution among the different nanofluids. The mid-height velocity profiles for different nanofluids are displayed in Figure 7 with Ra=10^6 and ϕ=4%. The velocity profiles show almost the same pattern for all type of nanofluids.

The effects of different nanofluids on the heat transfer rate are displayed in Figure 8. The figure obviously shows that the nanofluids provide higher rates of heat transfer than the pure fluid for all values of Rayleigh number. It is also observed that a better heat transfer rate is obtained upon using Ag nanofluid. A further scrutiny of the curves in Figure 8 reveals that the highest values of local Nusselt number are attained at Y=0.75 for Ra=10^6, i.e. ¾ from the bottom of the hot wall. In comparing isothermal wall and wall with linearly varying temperature, very different behaviour is observed. The highest local heat transfer rate is attained at the bottom portion of the hot wall for isothermal wall. However, the highest value of local Nusselt number is not attained at the bottom of the wall for wall with linearly varying temperature.

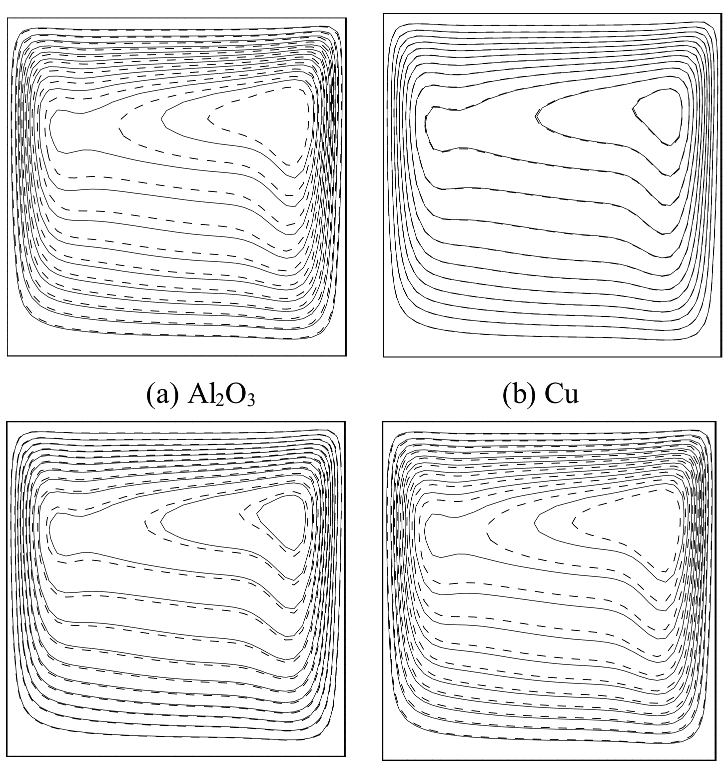

(a) Al_2O_3 (b) Cu

(c) Ag (d) TiO_2

Figure 5. Streamlines for pure fluid and different nanofluids (solid lines for pure fluid; dash lines for nanofluid) with Ra=10^6

Maejo Int. J. Sci. Technol. **2010**, *4*(03), 468-482

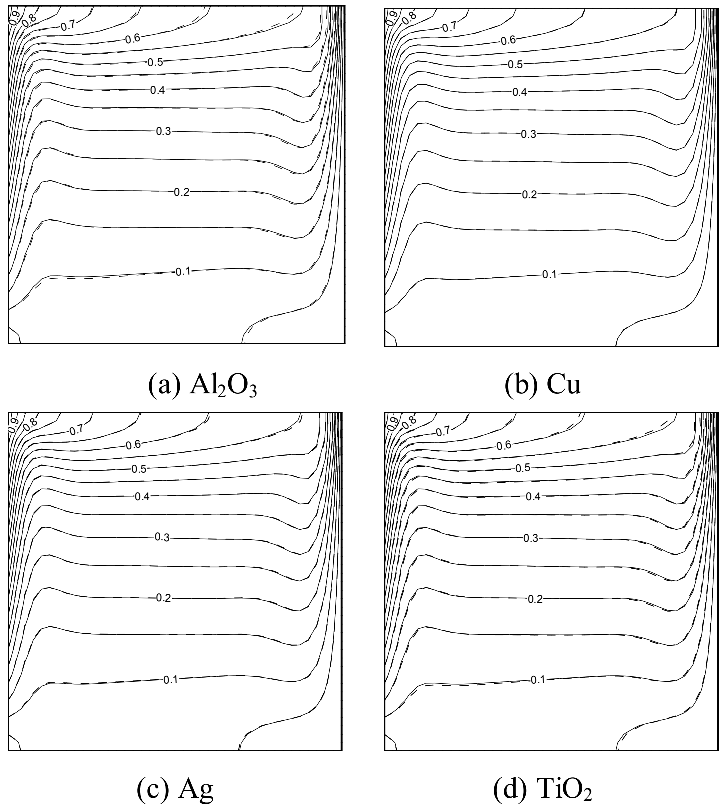

Figure 6. Isotherms for pure fluid and different nanofluids (solid lines for pure fluid; dash lines for nanofluid) with $Ra=10^6$

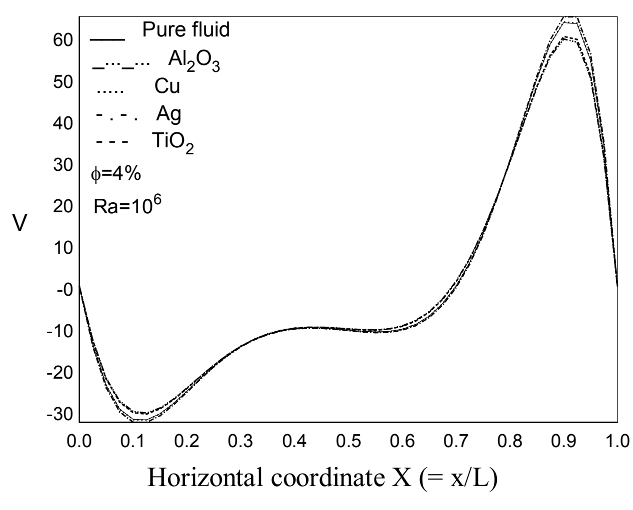

Figure 7. Mid-height velocity profiles for different nanofluids with $Ra=10^6$ and $\phi=4\%$

Maejo Int. J. Sci. Technol. **2010**, *4*(03), 468-482

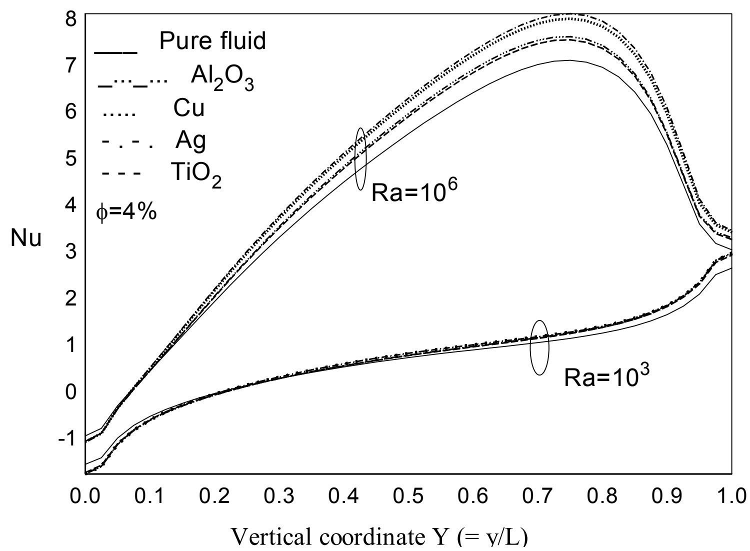

Figure 8. Local Nusselt number for different nanofluids with ϕ=4%

In order to find the effect of total heat transfer rate across the cavity among the different nanofluids, the average Nusselt number is plotted against the volume fraction of the nanoparticles for different values of Rayleigh number in Figure 9. The beneficial effects of the particle fraction on the average Nusselt number can be seen evidently with increasing the particle fraction. An increase in the average Nusselt number can be seen for all values of Rayleigh number. It is found that a maximum heat transfer rate is observed with Ag nanoparticles. When increasing the volume fraction of nanofluids, the difference in the heat transfer rate among the various nanofluids also increases. The difference among various nanoparticles provides a major effect on the convective heat transfer rate, which is clearly seen in Figure 9.

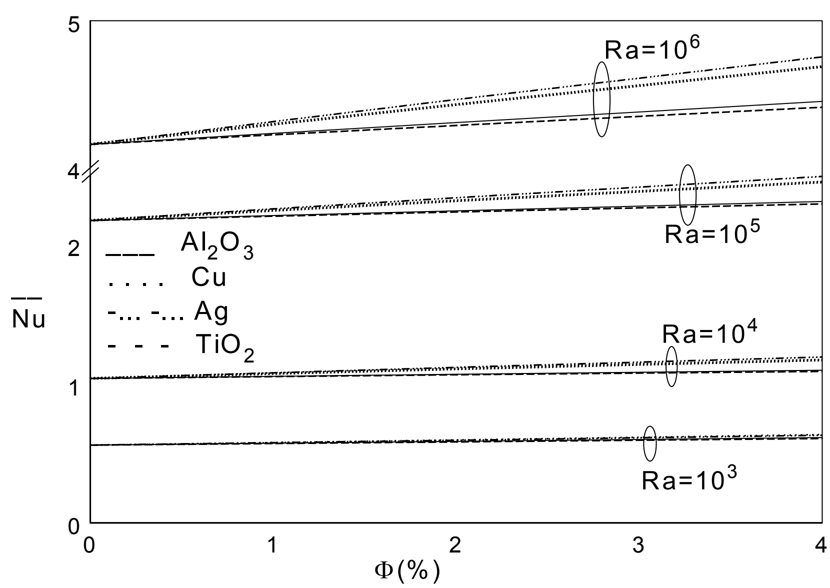

Figure 9. Average Nusselt number for different nanofluids and volume fractions

Maejo Int. J. Sci. Technol. **2010**, *4*(03), 468-482

Figure 10, which plots the heat transfer coefficient ratio (ε_h) against the Rayleigh number for different volume fractions of the nanoparticles, demonstrates the heat transfer efficacy of the nanofluids at different volume fractions of the nanoparticles. The heat transfer coefficient ratios of the oxide nanofluids (Al_2O_3 and TiO_2) reach a minimum when Ra=10^4. However, the opposite behaviour is observed when using metal particles (Cu and Ag)–a maximum heat transfer ratio is attained at Ra=10^4. It is also found that the heat transfer coefficient ratio is always above unity. The highest values of the heat transfer coefficient ratio for the oxide nanofluids are obtained for Ra=10^3, whereas those for the metal nanofluids are obtained for Ra=10^4.

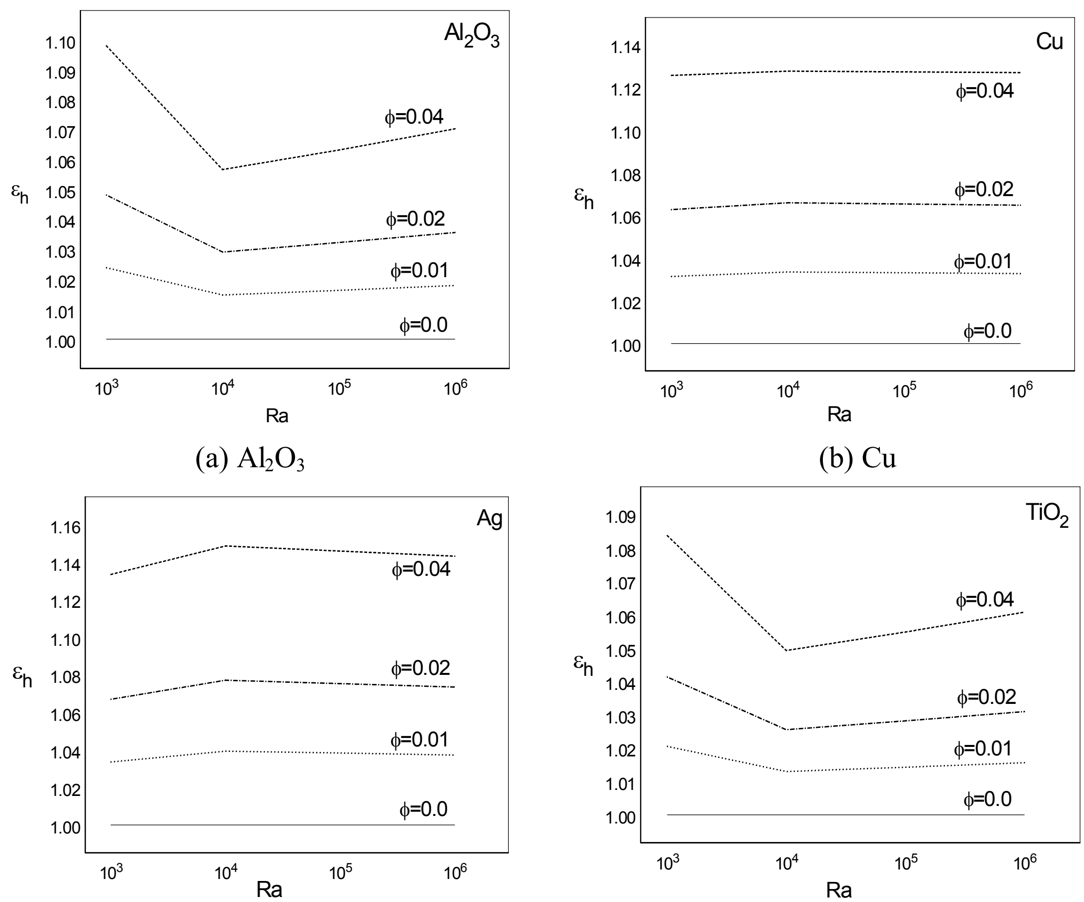

(a) Al_2O_3 (b) Cu

(c) Ag (d) TiO_2

Figure 10. Heat transfer coefficient ratio for different nanofluids

From the simulation results obtained for various parameters involved in this study, the following sets of figures can be enumerated. The average Nusselt number of nanofluids at 1% volume concentration of Al_2O_3, Cu, Ag and TiO_2 particles increases 2.4%, 3.2%, 3.4% and 2.1% respectively for Ra=10^3 compared with the base fluid. The heat transfer rate of nanofluids with 4% volume concentration of Al_2O_3, Cu, Ag and TiO_2 particles increases 9.8%, 12.6%, 13.4% and 8.4% respectively for Ra=10^3 compared with the base fluid. The average Nusselt number of nanofluids with 1% volume

Maejo Int. J. Sci. Technol. **2010**, *4*(03), 468-482

concentration of Al_2O_3, Cu, Ag and TiO_2 particles increases 1.8%, 3.3%, 3.7% and 1.6% respectively for Ra=10^6 compared with the base fluid. Heat transfer rate of nanofluids with 4% volume concentration of Al_2O_3, Cu, Ag and TiO_2 particles increases 7.0%, 12.7%, 14.3% and 6.1% respectively for Ra=10^6 compared with the base fluid. When increasing the Rayleigh number for a given volume fraction of nanoparticles, the average Nusselt number is constant for Cu nanofluid, while for Ag nanofluid a small amount of variation in the average Nusselt number is found. On the other hand, variation in the average Nusselt number is high for the nanofluids with Al_2O_3 and TiO_2 particles on the same conditions. Therefore, the choice of nanoparticles is very important in the convective heat transfer application.

CONCLUSIONS

The present study numerically examines the heat transfer enhancement of water-based nanofluids containing various nanoparticles in a square cavity with linearly varying wall temperature. Simulation results from a comparative study of four different nanoparticles (Al_2O_3, Cu, Ag and TiO_2) have been presented in detail. The heat transfer capacity of the base fluid can be increased by suspending the nanoparticles in it and the effect is more pronounced as the volume fraction of the particles increases. However, the incremental change in the average Nusselt number is strongly depending on the nanoparticles chosen. The linearly varying wall temperature changes the flow pattern and results in a higher heat transfer rate when compared to the isothermal wall. The heat transfer coefficient ratios of Al_2O_3 and TiO_2 nanofluids are minimum when Ra=10^4 while they are maximum for Cu and Ag nanofluids. Results clearly show that the type of nanoparticles considered is very important on the convective heat transfer application. A significant difference on the average Nusselt number is found for different nanoparticles.

REFERENCES

1. S. U. S. Choi and J. A. Eastman, "Enhancing thermal conductivity of fluids with nanoparticles", ASME International Mechanical Engineering Congress and Exposition, **1995**, San Fancisco, USA.
2. P. E. Phelan, P. Bhattacharya and R. S. Prasher, "Nanofluids for heat transfer applications", *Ann. Rev. Heat Transf.*, **2005**, *14*, 255-275.
3. S. Das, S. Choi and H. Patel, "Heat transfer in nanofluids – A review", *Heat Transf. Eng.*, **2006**, *27*, 3-19.
4. V. Trisaksri and S. Wongwises, "Critical review of heat transfer characteristics of nanofluids", *Renew. Sustain. Energy Rev.*, **2007**, *11*, 512-523.
5. X. Q. Wang and A. S. Mujumdar, "Heat transfer characteristics of nanofluids: A review", *Int. J. Thermal Sci.,* **2007**, *46*, 1-19.
6. K. Khanafer, K. Vafai and M. Lightstone, "Buoyancy-driven heat transfer enhancement in a two-dimensional enclosure utilizing nanofluids", *Int. J. Heat Mass Transf.*, **2003**, *46*, 3639-3653.
7. R. Y. Jou and S. C. Tzeng, "Numerical research of nature convective heat transfer enhancement filled with nanofluids in rectangular enclosures", *Int. Commun. Heat Mass Transf.*, **2006**, *33*, 727-736.

Maejo Int. J. Sci. Technol. **2010**, *4*(03), 468-482

8. D. Wen and Y Ding, "Natural convective heat transfer of suspensions of titanium dioxide nanoparticles (nanofluids) ", *IEEE Trans. Nanotechnol.*, **2006**, *5*, 220-227.
9. K. S. Hwang, J. H. Lee and S. P. Jang, "Buoyancy driven heat transfer of water-based Al_2O_3 nanofluids in a rectangular cavity", *Int. J. Heat Mass Transf.*, **2007**, *50*, 4003-4010.
10. C. J. Ho, M. W. Chen and Z. W. Li, "Numerical simulation of natural convection of nanofluid in a square enclosure: Effects due to uncertainties of viscosity and thermal conductivity", *Int. J. Heat Mass Transf.*, **2008**, *51*, 4506-4516.
11. E. Abu-Nada, Z. Masoud and A. Hijazi, "Natural convection heat transfer enhancement in horizontal concentric annuli using nanofluids", *Int. Comm. Heat Mass Transf.*, **2008**, *35*, 657-665.
12. H. F. Oztop and E. Abu-Nada, "Numerical study of natural convection in partially heated rectangular enclosures filled with nanofluids", *Int. J. Heat Fluid Flow*, **2008**, *29*, 1326-1336.
13. A. K. Santra, S. Sen and N. Chakraborty, "Study of heat transfer augmentation in a differentially heated square cavity using copper-water nanofluid", *Int. J. Thermal Sci.*, **2008**, *47*, 1113-1122.
14. B. Ghasemi and S. M. Aminossadati, "Natural convection heat transfer in an inclined enclosure filled with a water-CuO nanofluid", *Numer. Heat Transf. Part A*, **2009**, *55*, 807-823.
15. M. A. Hossain and M. Wilson, "Natural convection flow in a fluid-saturated porous medium enclosed by non-isothermal walls with heat generation", *Int. J. Therm. Sci.* **2002**, *41*, 447-454.
16. N. H. Saeid and Y. Yaacob, "Natural convection in a square cavity with spatial side-wall temperature variation", *Numer. Heat Transf., Part A*, **2006**, *49*, 683-697.
17. M. Sathiyamoorthy, T. Basak, S. Roy and I. Pop, "Steady natural convection flows in a square cavity with linearly heated side wall(s) ", *Int. J. Heat Mass Transf.*, **2007**, *50*, 766-775.
18. A. A. Dare and M. O. Petinrin, "Modelling of natural convection along isothermal plates and in channels using diffusion velocity method", *Maejo Int. J. Sci. Technol.*, **2010**, *4*, 43-52.
19. H. C. Brinkman, "The viscosity of concentrated suspensions and solution", *J. Chem. Phys.*, **1952**, *20*, 571-581.
20. S. V. Patankar, "Numerical Heat Transfer and Fluid Flow", Hemisphere, New York, **1980**, pp.79-135.
21. G. D. V. Davis, "Natural convection of air in a square cavity: A bench mark numerical solution", *Int. J. Numer. Meth. Fluids*, **1983**, *3*, 249-264.
22. G. V. Hadjisophocleous, A. C. M. Sousa and J. E. S. Venart, "Prediction of transient natural convection in enclosures of arbitrary geometry using a nonorthogonal numerical model", *Numer. Heat Transf., Part A*, **1988**, *13*, 373-392.
23. T. Fusegi, J. M. Hyun, K. Kuwahara and B. Farouk, "A numerical study of three-dimensional natural convection in a differentially heated cubical enclosure", *Int. J. Heat Mass Transf.*, **1991**, *34*, 1543-1557.
24. G. Barakos, E. Mitsoulis and D. Assimacopoulos, "Natural convection flow in a square cavity revisited: Laminar and turbulent models with wall functions", *Int. J. Numer. Meth. Fluids*, **1994**, *18*, 695-719.